Original Article

PREPARATION, CHARACTERIZATION, AND OPTIMIZATION OF MEBENDAZOLE SPHERICAL AGGLOMERATES USING MODIFIED EVAPORATIVE PRECIPITATION IN AQUEOUS SOLUTION (EPAS)

DHARMESHKUMAR M. MODI[a]* ID, AKSHAT D. MODI[b,c] ID, RAJESH H. PARIKH[d], JOLLY R. PARIKH[e]

[a]Gujarat Technological University, Ahmedabad, Gujarat 382424, India, [b]Department of Biological Sciences, University of Toronto Scarborough, Toronto, ON M1C 1A4, Canada, [c]Department of Genetics and Development, Krembil Research Institute, University Health Network, Toronto, ON M5T 2S8, Canada, [d]SICART, Vallabh Vidyanagar 388120 Gujarat India, [e]A R College of Pharmacy Andamp; G H Patel Institute of Pharmacy, Vallabh Vidyanagar 388120 Gujarat, India
Email: dharmesh1571@gmail.com

ABSTRACT

Objective: Mebendazole is a popular benzimidazole class anthelmintic drug useful in the treatment of main infections of threadworms as well as other less common worm infections like whipworm, roundworm, and hookworm in adults and children over 2 y of age. It is poorly soluble in water resulting in poor absorption from the intestinal tract leading to a decrease in bioavailability. Moreover, Mebendazole has poor flowability due to the needle-shaped crystals. This work was carried out with the aim of increasing the flowability and solubility of Mebendazole.

Methods: A 3^2 full factorial design was used to investigate the effect of the concentration of Mebendazole and the quantity of water as an external phase using evaporative precipitation into an aqueous solution. The prepared agglomerates were characterized for particle size distribution, shape, Hausner ratio, Carr's index and % dissolved in 60 min (C_{60}).

Results: The prepared agglomerates were found to be monodispersed. They also showed a decrease in the Hausner ration and Carr's index, indicating improved flowability. Increase in C_{60} indicated that the agglomerates were found to have increased water solubility.

Conclusion: Scanning Electron Microscopy showed that the agglomerates were spherical in shape. Fourier Transformed Infra-Red studies showed no chemical change in the prepared spherical agglomerates. Differential Scanning Calorimetry and X-ray diffraction studies showed an increase in amorphous characteristics of prepared spherical agglomerates. This method may be used for drugs with similar characteristics as Mebendazole.

Keywords: Mebendazole, EPAS, Spherical agglomerates, Uniformity index, Desirability function, Flow ability, Compressibility, Dissolution

INTRODUCTION

Mebendazole (MBZ) is a synthetic popular benzimidazole class anthelmintic drug useful in the treatment of main infections of threadworms as well as other less common worm infections like whipworm, roundworm, and hookworm in adults and children over 2 y of age [1, 2]. MBZ shows great promise in the treatment of capillariasis and hydatid disease. It has recently shown efficacy as an anticancer agent [3]. Through microtubular destruction, mebendazole kills helminths by inhibiting glucose uptake into susceptible parasites [4]. MBZ belongs to class II of the biopharmaceutics classification systems (BCS) as it is poorly soluble in water and slow to dissolve [5-9]. It results in poor absorption from the intestinal tract [10]. Its systemic efficacy is limited by its poor water solubility [11]. MBZ has poor flowability due to needle-shaped crystals [8].

Spherical agglomeration is a novel particle engineering technique in which spherical particles of amorphous nature can be obtained by various spherical agglomeration methods in the same process. Spherical shape leads to enhanced flowability, compressibility, and amorphousness, increases the solubility in water. Spherical agglomerates can be obtained by typical spherical crystallization techniques like wet spherical agglomeration method, quasi emulsion solvent diffusion (QESD) method [12, 13], ammonia diffusion method [14], neutralization method [15], crystal co-agglomeration method [16]; non-typical spherical crystallization techniques like cooling method, pH method, salting out method, and other techniques [17] like evaporative precipitation into aqueous solutions (EPAS) [18], solution atomization and crystallization by sonication (SAXS) [19-22], solvent evaporation method [23, 24].

The objective of the present study is to enhance the flowability and solubility of MBZ by preparing spherical agglomerates through evaporative precipitation into an aqueous solution (EPAS).

MATERIALS AND METHODS

Materials

MBZ was received as a gift sample from K A Malle Pharmaceuticals Ltd (Ankleshwar, Gujarat, India). Formic acid AR grade was purchased from SD Fine Chem Limited (Mumbai, India). Distilled deionized water purchased from SICART (Vallabh Vidyanagar, India) was used throughout the study.

Preparation of spherical agglomerates

A fixed amount of MBZ is dissolved in 1 ml of formic acid to prepare the solution. The MBZ solution was sprayed at a rate of 1 ml/min using the spray gun into the water at 90 C and stirred at 600 rpm using a magnetic stirrer. The stirring continued for a further 3 min after the complete addition of MBZ solution. The particles of MBZ obtained in the water were separated by vacuum filtration (Erection Engineering, India). Particles were washed with water (25 ml each 3 times) to make them free from formic acid.

Preparation of batches

The factors like concentration of MBZ and volume of external phase (water) affecting the spherical agglomeration were chosen at different three levels as shown in table 1 with coded and actual values.
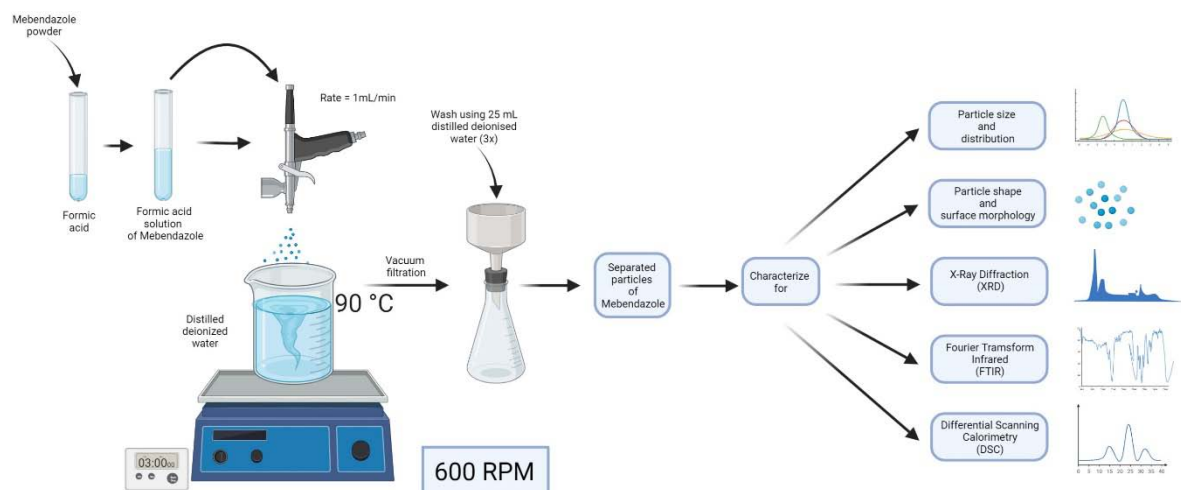
Fig. 1: The graphical abstract for preparation of spherical agglomerates

Table 1: Levels of independent variables for 32 factorial designs

S. No.	Independent variable	Low level (-1)	Medium level (0)	High level (1)
1	Concentration of MBZ (X1)	2.5%	7.5%	12.5%
2	The volume of the external phase (X2)	25ml	50ml	75ml

A 3^2 full factorial design was applied to optimize these process variables. The composition of all the above nine batches is shown in table 2. All nine batches were prepared in triplicate.

Table 2: Composition of various batches of mebendazole spherical agglomerates

	Transformed values		Real values	
Batch No.	Concentration of drug (X1)	The volume of external phase (ml) (X2)	Concentration of drug (X1)	The volume of external phase (ml) (X2)
E1	-1	-1	2.5 %	25
E2	-1	0	2.5 %	50
E3	-1	1	2.5 %	75
E4	0	-1	7.5 %	25
E5	0	0	7.5 %	50
E6	0	1	7.5 %	75
E7	1	-1	12.5 %	25
E8	1	0	12.5%	50
E9	1	1	12.5%	75

Characterization of spherical agglomerates particle size analysis

The particle size and distribution of pure MBZ and processed MBZ were determined by laser diffraction. The wet sample was fed into a HELOS laser diffraction sensor (HELOS/BF; GmbH, Germany). Measurement of the median particle size distribution (x50) defined by the Volume Mean Diameter (VMD) was made.

Uniformity index

It was calculated by using the following formulae

$$UI = \frac{Dw}{Dn}$$

Where Dw and Dn are average weight diameter and average number diameter respectively and are calculated as follows

$$Dw = \frac{\sum NiDi4}{\sum NiDi3}$$

$$Dn = \frac{\sum NiDi}{\sum Ni}$$

Where Ni is the number of particles with Di diameter

The values of UI ranging from 1.0 to 1.1 and 1.1 to 1.2 indicate monodisperse and nearly monodisperse particles [25].

Flowability and compressibility

The bulk density (BD) and tapped density (TD) densities were determined using the standardized method as described in the United States Pharmacopoeia (Bulk density test apparatus; Erection, India). A fixed amount of powder was poured into a cylinder and the level was recorded. The sample was subjected to 2500 mechanical tapping and the TD was determined using the tapped volume. In addition, these measurements, the Hausner ratio, as an indicator of flowability and cohesiveness as well as Carr's index, as an indicator of compressibility as previously described, were calculated.

Drug dissolution study

The dissolution study was performed using USP type II device DA-6 (Veego Scientific, Mumbai) under non-sink conditions. A 100 mg of pure or processed MBZ powder sample was placed in 500 ml of distilled deionized water as a dissolution medium at 37±0.5 °C and stirred at 100 rpm. The 5 ml samples were withdrawn and filtered through 0.45 μm filters (Whatman filters, USA). The samples were withdrawn at 5,10,15,30,45, and 60 min with media replacement. The % of dissolved MBZ was determined and designated as C60.

% Yield calculation

% Yield was calculated by weighing the total amount of MBZ powder obtained for each batch divided by the total amount of MBZ powder

taken for the process as per the following formulae.

$$\% \text{ yield} = \frac{\text{Weight of treated MBZ powder}}{\text{Weight of MBZ powder taken}} \times 100$$

Surface morphology

Scanning electron microscopy (SEM; XL 30; Philips, Netherlands) was used to examine the surface morphologies of the MBZ and treated MBZ powder particles. All the samples were gold-palladium sputtered before analysis, and SEM was carried out at 5 kV.

Powder X-ray diffraction (PXRD)

The phase of the MBZ and processed MBZ particles was analyzed using an Xpert MPD diffractometer (Philips, Holland).

Fourier-transform infrared spectroscopy (FTIR)

FTIR spectra of MBZ and treated MBZ powder were recorded over a wavelength of 400 cm-1 to 4000 cm-1 using Spectrum GX spectrophotometer (Perkin Elmer, Germany) using an attenuated total reflectance (ATR) mode.

Differential scanning calorimetry (DSC)

The DSC analysis was performed using Pyris-1 DSC (Perkin Elmer, Germany) differential scanning calorimeter. The materials samples (10 mg) were weighed to aluminum pans (25 l) and sealed with pierced lids. The analysis was performed in the temperature range of 0 to 500 °C in a nitrogen atmosphere (50 ml min^{-1}) using a heating rate of 5 °C min^{-1}. An empty pan sealed with a pierced lid was used as a reference.

Multivariate data analysis

The effects of independent variables and their interaction on the results of Hausner ratio, Carr's index, and C60 values were analyzed; the data were subjected to multiple regression, and a statistical model incorporating interactive and polynomial terms shown in equation 1 was used to evaluate the response by using the Design Expert® 7.1.6 software

$$Y_i = b_0 + b_1 X_1 + b_2 X_2 + b_{11} X_{11} + b_{22} X_{22} + b_{12} X_1 X_2 \ldots\ldots (1)$$

Where Y_i is the dependent variable; b_0 is the arithmetic mean of the 9 terms; b_i is the estimated coefficient for the factor X_i.

An equation was proposed for every dependent variable to determine coefficients and the p values of each term of the derived equation. The multiple regression of significant terms and dependent variables gives the reduced model equation.

Contour plots

The effect of the two independent variables on the Hausner ratio, Carr's index, and C60 was optimized by generating the contour plots using the Design Expert® 7.1.6 software, and various values of them were found to give the optimized product.

Selection of the best batch

During the optimization of a multivariable process, in spherical agglomeration, the responses have to be combined to produce a product of desired characteristics. The application of the desirability function combines all the responses in one measurement and gives the possibility to predict the optimum levels of the independent variables.

Individual desirability for each response (ID) is calculated from the following equation.

$$ID = \frac{Q}{R\max - R\min}$$

Q = Rmax–R OR Q = R–Rmin

Here, Q = difference obtained by subtracting an individual response from the maximum or the minimum value of the response

Rmax = maximum value of the response from all response values
Rmin = minimum value of the response from all response values

R = value of the response experimentally determined. Overall desirability (OD) is calculated from the following equation.

$$OD = (ID_1 \times ID_2 \times ID_3)^{1/3}$$

The value of OD near 1 indicates the batch or product has all the different desired characteristics [26].

The best batch was selected and further analyzed for SEM, XRD, FTIR, and DSC to check for sphericity, crystalline or amorphous characteristics, as well as any change in chemical composition.

Checkpoint analysis

A checkpoint analysis was performed to confirm the role of derived polynomial equations in predicting the responses. Values of independent variables were taken at 2 points as shown in table 3. The theoretical values for HR, % C and C60 were calculated by substituting the values in the polynomial equation. Spherical agglomerates were prepared experimentally at 2 checkpoints and transformed for the responses.

Table 3: Composition of checkpoint batches

Checkpoint batch	X1	X2
C1	0.7	-0.5
C2	-1.2	1.1

RESULTS AND DISCUSSION

Characterization of spherical agglomerates

The characteristics of MBZ and different batches of spherical agglomerates are shown in table 4.

Table 4: Characteristics of MBZ and different batches of spherical agglomerates

Batch no.	Particle size* (µm)	UI	HR#	%C#	C60#	Yield#
MBZ	14.6	1.58	1.60+0.01	37.50+0.45	50.50+0.4	—
E1	28.7	1.36	1.32+0.04	24.24+0.32	63.1+0.3	63+2
E2	35.6	1.40	1.45+0.02	31.03+0.02	62.2+0.5	62+4
E3	42.1	1.52	1.43+0.07	30.07+0.08	60.2+0.01	61+2
E4	39.8	1.48	1.30+0.06	23.08+0.12	66.3+0.3	62+1
E5	44.6	1.42	1.34+0.04	25.37+0.31	62.4+0.07	61+2
E6	52.3	1.39	1.38+0.05	27.54+0.06	61.3+0.2	63+1
E7	55.3	1.43	1.28+0.09	21.88+0.00	71.5+0.03	62+2
E8	35.6	1.48	1.32+0.03	24.24+0.04	68.6+0.6	64+3
E9	44.5	1.53	1.36+0.04	26.47+0.06	64.4+0.4	63+1

Here* Volume Mean Diameter (VMD)# mean±SD (n = 3); UI = Uniformity index; HR = Hausner Ratio; %C = Carr's compressibility index; C60 = % drug dissolved in 60 min

The mean volume diameter of the prepared agglomerates has been increased, indicating that the agglomeration of particles has taken place.

The UI of spherical agglomerates was always less than that of MBZ. This indicates that the process helps in narrowing particle size distribution.

However, all the batches of spherical agglomerates exhibit UI greater than 1.2 (maximum 1.53). Thus, the particle size distribution of spherical agglomerates may be described as nearly monodisperse [27, 28].

The yield of various batches was found in the range of 61-64%. It indicates that the process is giving a good yield, but the process may be further improved to obtain a yield close to 100%.

Effect on flowability

A quadratic equation (full model) was obtained for HR and %C as,

$$HR = 1.3567 - 0.04X_1 + 0.045X_2 + 0.02X_{12} - 0.025X_{22} - 0.0075X_1X_2 \ldots\ldots (2)$$

$$\% C = 26.2189 - 2.125X_1 + 2.48X_2 + 0.9917X_{12} + 1.333X_{22} - 0.31X_1X_2 \ldots\ldots (3)$$

The correlation coefficient (r^2) of HR and % C was found to be 0.9032 and 0.9132, respectively, indicating a good fit. The main effects of X1 and X2 represent the average result of changing one variable at a time from its low to high value. The interaction terms show how HR and %C values are affected when two or more variables were simultaneously changed. Equations 2 and 3 represent the effects of individual and combined variables on HR and %C of prepared spherical agglomerates, respectively. The values of coefficients of X12, X22, and X1X2 (having p>0.05) in equation 2 and the value of coefficients X12, X22, and X1X2 (having p>0.05) in equation 3 are regarded as the least contributing factors and hence, these terms were neglected to develop a reduced model (equation 4 and 5) by multiple regression of the significant terms (p<0.05) as,

$$HR = 1.3567 - 0.04X_1 + 0.045X_2 - 0.025X_{22} \ldots\ldots (4)$$

$$\% C = 26.2189 - 2.125X_1 + 2.48X_2 \ldots\ldots (5)$$

F-statistics of the results of the full model and reduced model ANOVA confirmed the omission of insignificant terms from equations 2 and 3 as F calculated value is less than F tabled value. So, the neglected terms do not significantly contribute to predicting the HR and %C of MBZ spherical agglomerates. It is evident from equations 4 and 5 that spherical agglomerates with good flowability (low value of HR and %C) can be prepared by taking a high concentration of drugs and a low volume of water.

Effect on dissolution

A quadratic equation (full model) was obtained for % drug dissolved in 60 min C60 as,

$$C60 = 63.2889 + 3.1667X_1 - 2.5X_2 + 1.6667X_{12} + 0.0667X_{22} - 1.05X_1X_2$$

$$\ldots\ldots (6)$$

The value of the correlation coefficient (r^2) was found to be 0.9918, indicating a good fit. The main effects of X1 and X2 represent the average result of changing one variable at a time from its low to high value. The interaction terms show how C60 values are affected when two or more variables were simultaneously changed. Equation 6 represents the effects of individual and combined variables on the C60 of the prepared spherical agglomerates. The values of coefficients of X22 (having p>0.05) in equation 6 are regarded as the least contributing factors and hence, these terms were neglected to develop a reduced model (equation 7) by multiple regression of the significant terms (p<0.05) as,

$$C60 = 63.2889 + 3.1667X_1 - 2.5X_2 \ldots\ldots (7)$$

F-statistics of the results of ANOVA of the full model and reduced model confirmed the omission of insignificant terms from equation 6 as F calculated value if less than the F tabled value. So, the neglected terms do not significantly contribute to predicting the C60 of MBZ spherical agglomerates.

During dissolution studies, it was observed that the unprocessed MBZ initially floated on the surface of the dissolution medium while the modified EPAS-processed powders were wetted readily and quickly dissolved [29-32].

It is evident from the equation that spherical agglomerates with good dissolution (high value of C60) can be prepared by taking a higher amount of drug and a lower volume of water. This may be attributed to a decrease in the crystallinity of MBZ.

Contour plots

Contour plots generated from Design Expert software are shown in fig. 1, 2, and 3; HR, %C, and C60 are indicated, respectively. It was observed from the contour plot fig. 1 that the lowest value of HR (1.3) could be obtained with X1 between-0.5 level (5%) to 0.5 level (10%) and X2 between 0.5 level (62.5 ml) to 1 level (75 ml). Fig. 2 revealed that the lowest value of % C (24) could be obtained with X1 between-0.5 level (5%) to 0.5 level (10%) and X2 between 0.5 level (62.5 ml) to 1 level (75 ml). Fig. 3 showed that the maximum value of C60 (70%) could be obtained with X1 between 0.5 level (10%) to 1 level (12.5%) and X2 between 0 levels (50 ml) to 1 level (75 ml). All the two-dimensional contour plots were found to follow the nonlinear relationship between X1 and X2 variables. From the contour, it was observed that drug concentration (10%) and higher volume of external phase (75 ml) are necessary for lowest HR and %C as well as highest C60.
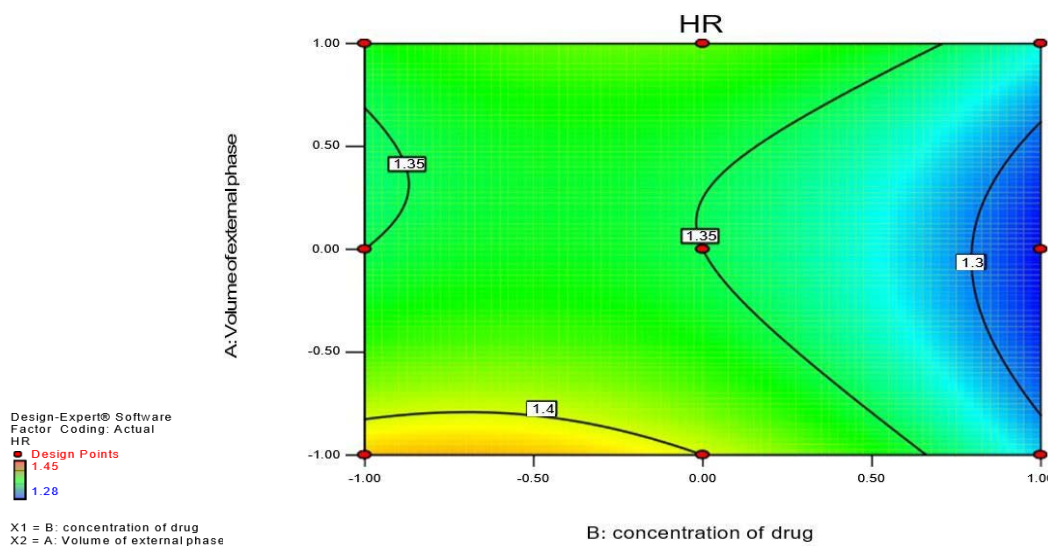
Fig. 2: Contour plot showing the effect of X1 and X2 on HR
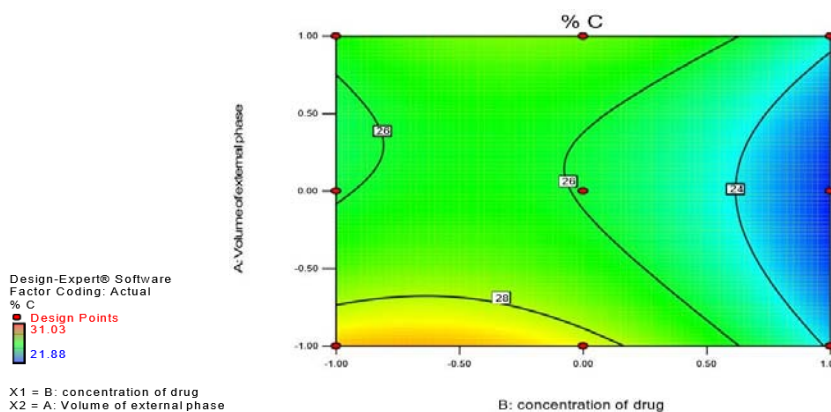
Fig. 3: Contour plot showing the effect of X1 and X2 on %C

Table 5: The individual and overall desirability of all batches

Batch No	ID1	ID2	ID3	OD
E1	0.765	0.742	0.257	0.526
E2	0	0	0.177	0
E3	0.118	0.105	0	0
E4	0.882	0.869	0.540	0.745
E5	0.647	0.619	0.195	0.427
E6	0.412	0.381	0.097	0.248
E7	1	1	1	1
E8	0.765	0.742	0.743	0.750
E9	0.529	0.498	0.372	0.461

Here, ID= Individual Desirability; OD= Overall Desirability
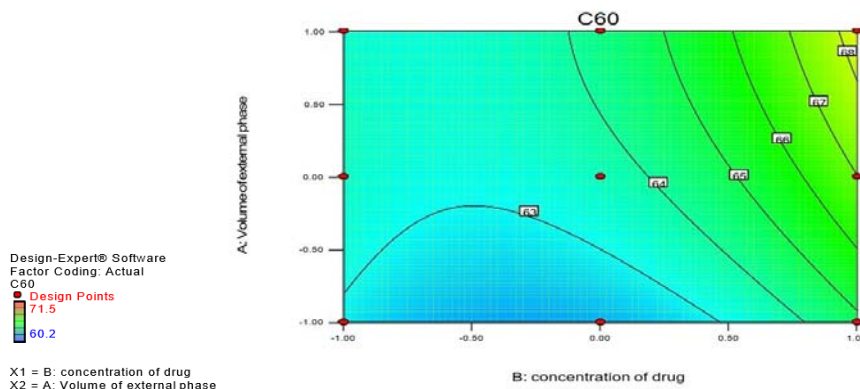
Fig. 4: Contour plot showing the effect of X1 and X2 on C60Selection of the best batch

The values of individual desirability ID1, ID2, ID3, and overall desirability OD for every batch are shown in table 5. It is evident from the table that batch E7 has the highest OD value. This can be called the best batch among all 9 batches prepared.

Checkpoint analysis

From the contour plot, two sets of X1 and X2 were selected. The spherical agglomerates of MBZ were prepared experimentally using the same procedure keeping the other process variables constant with the amounts of X1 and X2 at the selected checkpoint. The experiment was repeated three times and experimentally obtained mean HR, %C and C60 values compared with the predetermined values. The values are also determined from the respective contour plot for batches C1 and C2. All values are shown in table 6. No significant difference ($p > 0.05$) was observed between calculated and experimental values of HR, %C, and C60.

Table 6: Calculated and experimentally determined values for the checkpoint batches

Checkpoint batch	HR		% C		C60	
	Calcu	Experi	Calcu	Experi	Calcu	Experi
C1	1.35	1.33	25.98	25.7	64.26	63.9
C2	1.45	1.44	31.5	31.0	56.74	55.90

Mechanism of formation of spherical agglomerates and factors affecting the sphericity

We propose the following mechanism for the formation of spherical

agglomerates through the modified EPAS method [33-36].

- Formic acid (Internal phase) and water (external phase) are miscible.

- When the heated formic acid solution is sprayed into the aqueous solution as a powerful spray mist resulted in very fine formic acid droplets are formed. Very rapid evaporation of the heated organic solution in EPAS results in fast nucleation, resulting in an amorphous nanoparticle suspension producing high super saturation of MBZ, thus favoring smaller spherical particles by stirring. It can be expected to bring about a high nucleation rate.

- At the end of spraying, a few small particles can be observed in the white opaque colloidal suspension. As water solubility of MBZ increases with temperature, some MBZ precipitates during cooling, increasing the particle size in the suspension.

Agglomerates are spherical in shape as evident from micrographs as shown in fig. 4.
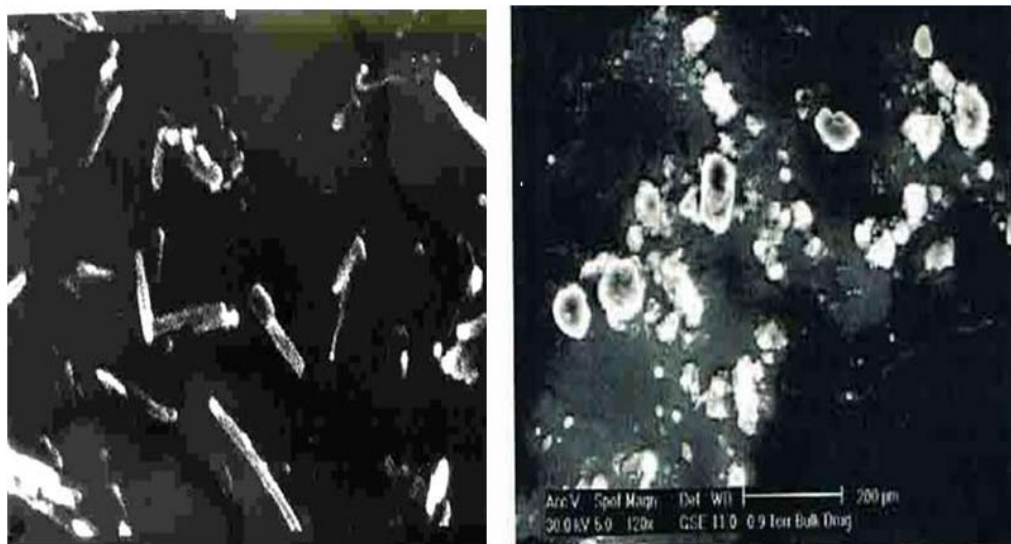
Fig. 5: SEM image of (A) pure MBZ and (B) batch E7

The process does not induce any chemical change in MBZ as evident from the comparison of FTIR spectra of MBZ and the agglomerates prepared from MBZ in fig. 5.

X-ray diffractograms of spherical agglomerates showed a similar number of peaks to that of the x-ray diffractogram of pure MBZ

but of lower intensity as per fig. 6. Besides this, the % reduction in the height of the peak of spherical agglomerates for pure MBZ is given in table 7. So, it is concluded that MBZ gets transformed to a less crystalline form during the spherical agglomeration process [37-39].
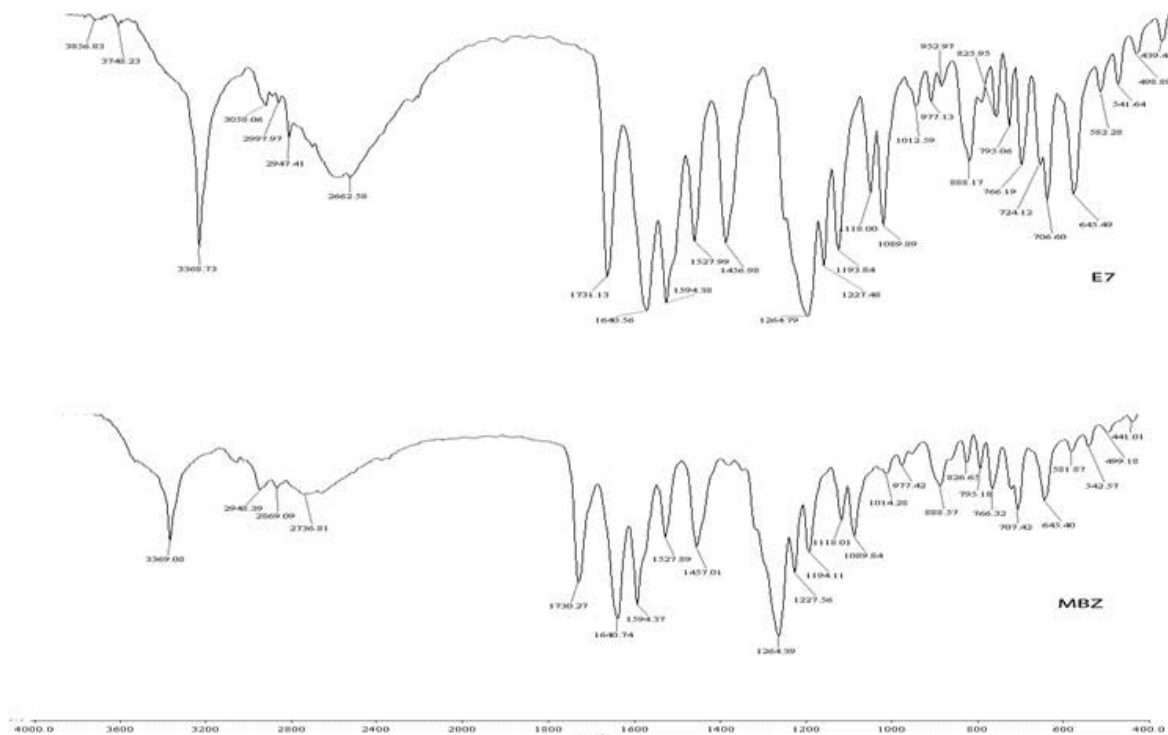
Fig, 6: FTIR spectra of pure mebendazole and spherical agglomerates of batch E7
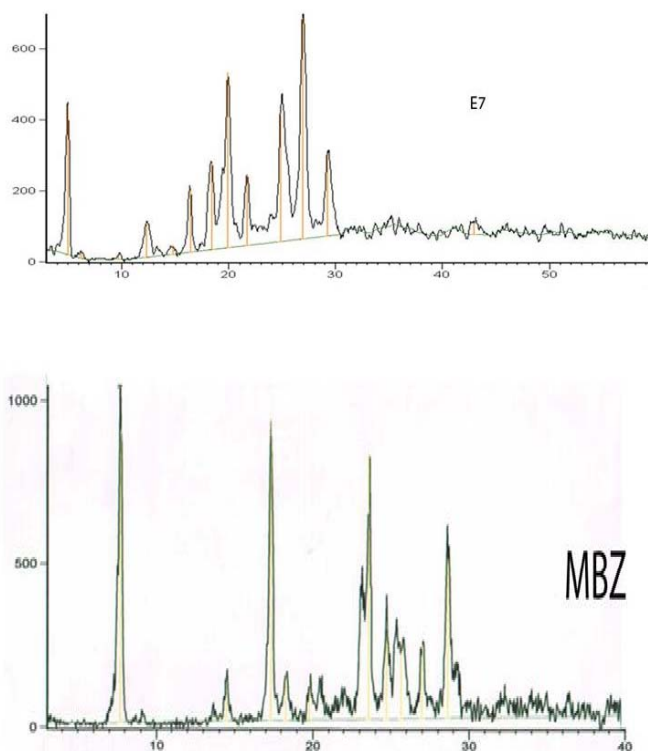
Fig. 7: X-ray diffractogram of pure MBZ and spherical agglomerates of batch E7
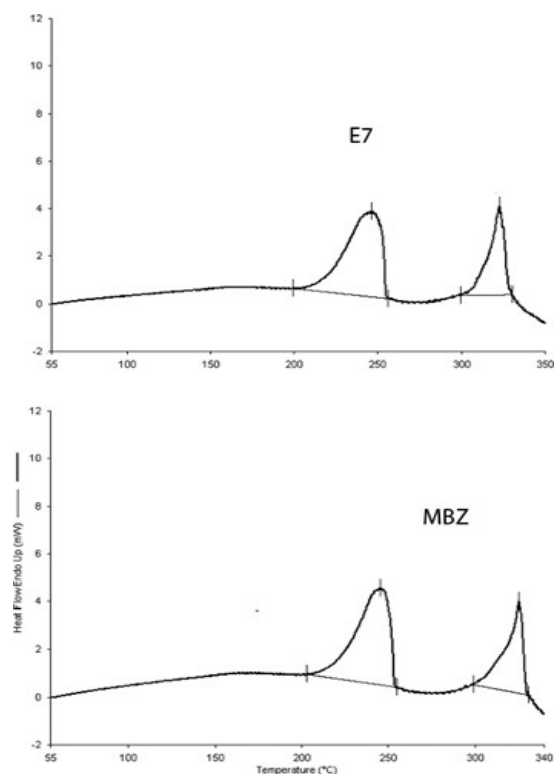
Fig. 8: DSC thermograms of pure MBZ and spherical agglomerates of batch E7

Table 7: % Reduction in the height of peaks at specific [2 Theta] values of pure MBZ and batch E7

Position [2 Theta] of MBZ	Position [2Theta]of Spherical agglomerates of batch E7	Height of pure MBZ	Height of spherical agglomerates of batch E7	% Reduction in height of a peak
14.4758	14.7968	128.61	22/58	82.44

DSC thermograms of pure MBZ and spherical agglomerates are depicted in fig. 7. Pure MBZ showed two endotherms at 245.286 °C and 325.574 °C, whereas the spherical agglomerates of the batch E7 showed at 246.098 °C and 322.72 °C as well as a decrease in the delta H values indicating that the pure MBZ has been transformed into the less crystalline form [37].

CONCLUSION

The study aimed to prepare, characterize, and optimize the spherical agglomerates of Mebendazole by evaporative precipitation into the aqueous solution (EPAS) method. This method uses the spraying of a formic acid solution of Mebendazole into poor solvent-water at 90 °C, which can remove the formic acid from droplets to make spherical particles and convert it into amorphous characteristics. By optimizing the various process parameters, the flowability, compressibility, and solubility were improved to the extent that made them suitable for direct processing to convert into tablets.

CONTRIBUTION OF AUTHORS

Dharmeshkumar M Modi carried out practical work, writing and revising the manuscript. Akshat D. Modi helped in writing and revising the manuscript. Rajesh H. Parikh guided and supervised the practical work along with the framing of the manuscript. Jolly R. Parikh guided and supervised the practical work along with the framing of the manuscript.

CONFLICT OF INTERESTS

The authors declare that they have no known competing financial interests or personal relationships that could have appeared to influence the work reported in this paper.

REFERENCES

1. Rakel RE. Conn's current therapy. W B Saunders; 1987.
2. Goodman and Gilman's the pharmacological basis of therapeutics. McGraw-Hill, Health Professions Division; 1996.
3. Zimmermann SC, Tichy T, Vavra J, Dash RP, Slusher CE, Gadiano AJ. N-substituted prodrugs of mebendazole provide improved aqueous solubility and oral bioavailability in mice and dogs. J Med Chem. 2018;61(9):3918-29. doi: 10.1021/acs.jmedchem.7b01792, PMID 29648826.
4. Keystone JS, Murdoch JK. Mebendazole. Ann Intern Med. 1979;91(4):582-6. doi: 10.7326/0003-4819-91-4-582, PMID 484964.
5. Shehatta I. Cyclodextrins as enhancers of the aqueous solubility of the anthelmintic drug mebendazole: thermodynamic considerations. Monatshefte Chem/Chemical. 2002;133(9):1239-47. doi: 10.1007/s007060200096.
6. Kipp JE. The role of solid nanoparticle technology in the parenteral delivery of poorly water-soluble drugs. Int J Pharm.

2004;284(1-2):109-22. doi: 10.1016/j.ijpharm.2004.07.019, PMID 15454302.

7. Hashimoto N, Yuminoki K, Takeuchi H, Okada C. Development of nanocrystal formulation of mebendazole with improved dissolution and pharmacokinetic behaviors. Asian J Pharm Sci. 2016;11(1):122-3. doi: 10.1016/j.ajps.2015.11.096.

8. Calvo NL, Kaufman TS, Maggio RM. Mebendazole crystal forms in tablet formulations. An ATR-FTIR/chemometrics approach to polymorph assignment. J Pharm Biomed Anal. 2016;122:157-65. doi: 10.1016/j.jpba.2016.01.035, PMID 26874854.

9. Parakh DR, Patil MP, Dashputre NL, Kshirsagar SJ. Development of self-micro emulsifying drug delivery system of mebendazole by spray drying technology: characterization, *in vitro* and *in vivo* evaluation. Drying Technol. 2016;34(9):1023-42. doi: 10.1080/07373937.2015.1090447.

10. Saidman E, Chattah AK, Aragon L, Sancho M, Cami G, Garnero C. Inclusion complexes of β-cyclodextrin and polymorphs of mebendazole: physicochemical characterization. Eur J Pharm Sci. 2019;127:330-8. doi: 10.1016/j.ejps.2018.11.012, PMID 30445224.

11. Lahiani Skiba M, Coquard A, Bounoure F, Verite P, Arnaud P, Skiba M. Mebendazole complexes with various cyclodextrins: preparation and physicochemical characterization. J Incl Phenom Macrocycl Chem. 2007;57(1-4):197-201. doi: 10.1007/s10847-006-9196-9.

12. Di Martino P, Di Cristofaro R, Barthelemy C, Joiris E, Palmieri Filippo G, Sante M. Improved compression properties of propyphenazone spherical crystals. Int J Pharm. 2000;197(1-2):95-106. doi: 10.1016/s0378-5173(99)00455-x, PMID 10704797.

13. Bethea ED, Gaj K, Gustafson JL, Axtell A, Lebeis T, Schoenike M. Pre-emptive pangenotypic direct-acting antiviral therapy in donor HCV-positive to recipient HCV-negative heart transplantation: an open-label study. Lancet Gastroenterol Hepatol. 2019;4(10):771-80. doi: 10.1016/S2468-1253(19)30240-7, PMID 31353243.

14. Puechagut HG, Bianchotti J, Chiale CA. Preparation of norfloxacin spherical agglomerates using the ammonia diffusion system. J Pharm Sci. 1998;87(4):519-23. doi: 10.1021/js960463w, PMID 9548908.

15. Swain S, Patra CN, Bhanoji Rao ME. Pharmaceutical drug delivery systems and vehicles. Woodhead Publishing India Pvt Ltd; 2016.

16. Jadhav N, Pawar A, Paradkar A. Design and evaluation of deformable talc agglomerates prepared by crystallo-Co-agglomeration technique for generating heterogeneous matrix. AAPS PharmSciTech. 2007;8(3):E59. doi: 10.1208/pt0803059, PMID 17915809.

17. Modi D, Parikh RH, Parikh JR. Novel Particle Engineering Techniques in Drug Delivery: Review of Coformulations Using Supercritical Fluids and Liquefied Gases; 2004;32:41-56.

18. Sarkari M, Brown J, Chen X, Swinnea S, Williams RO, Johnston KP. Enhanced drug dissolution using evaporative precipitation into aqueous solution. Int J Pharm. 2002;243(1-2):17-31. doi: 10.1016/s0378-5173(02)00072-8, PMID 12176292.

19. Kaerger JS, Edge S, Price R. Influence of particle size and shape on flowability and compactibility of binary mixtures of paracetamol and microcrystalline cellulose. Eur J Pharm Sci. 2004;22(2-3):173-9. doi: 10.1016/j.ejps.2004.03.005, PMID 15158902.

20. Ruecroft G, Hipkiss D, Ly T, Maxted N, Cains PW. Sonocrystallization: the use of ultrasound for improved industrial crystallization. Org Process Res Dev. 2005;9(6):923-32. doi: 10.1021/op050109x.

21. Rajadhyax A, Shinde U, Desai H, Mane S. Hot Mmelt extrusion in the engineering of drug cocrystals: a review. Asian J Pharm Clin Res 2021;14:10-9. doi: 10.22159/ajpcr.2021.v14i8.41857.

22. Dn CP, AS. A solubility enhancement of Acelofenac by new crystallization technique. Asian J Pharm Clin Res. 2021:113-8.

23. Alex R, Bodmeier R. Encapsulation of water-soluble drugs by a modified solvent evaporation method. I. Effect of process and formulation variables on drug entrapment. Journal of

Microencapsulation. 1990;7(3):347-55. doi: 10.3109/02652049009021845, PMID 2384837.

24. O'Donnell PB, McGinity JW, McGinity JW, O'Donnell PB. Preparation of microspheres by the solvent evaporation technique. Advanced Drug Delivery Reviews. 1997;28(1):25-42. doi: 10.1016/s0169-409x(97)00049-5, PMID 10837563.

25. Shukla PG, Kalidhass B, Shah A, Palaskar DV. Preparation and characterization of microcapsules of water-soluble pesticide monocrotophos using polyurethane as carrier material. Journal of Microencapsulation. 2002;19(3):293-304. doi: 10.1080/02652040110081343, PMID 12022495.

26. Swanepoel E, Liebenberg W, Devarakonda B, de Villiers MM. Developing a discriminating dissolution test for three mebendazole polymorphs based on solubility differences. Pharmazie. 2003;58(2):117-21. PMID 12641328.

27. Chen X, Vaughn JM, Yacaman MJ, Williams RO, Johnston KP. Rapid dissolution of high-potency danazol particles produced by evaporative precipitation into aqueous solution. J Pharm Sci. 2004;93(7):1867-78. doi: 10.1002/jps.20001, PMID 15176074.

28. Szunyogh T, Ambrus R, Szabo Revesz P. Formation of niflumic acid particle size by solvent diffusion and solvent evaporation as precipitation methods. Journal of Drug Delivery Science and Technology. 2012;22(4):307-12. doi: 10.1016/S1773-2247(12)50052-3.

29. Vaughn JM, McConville JT, Crisp MT, Johnston KP, Williams RO. Supersaturation produces high bioavailability of amorphous danazol particles formed by evaporative precipitation into an aqueous solution and spray freezing into liquid technologies. Drug Development and Industrial Pharmacy. 2006;32(5):559-67. doi: 10.1080/03639040500529176, PMID 16720411.

30. Gao L, Liu G, Wang X, Liu F, Xu Y, Ma J. Preparation of a chemically stable quercetin formulation using nanosuspension technology. International Journal of Pharmaceutics. 2011;404(1-2):231-7. doi: 10.1016/j.ijpharm.2010.11.009, PMID 21093559.

31. Alshora DH, Ibrahim MA, Alanazi FK. Nanotechnology from particle size reduction to enhancing aqueous solubility. In: Surface chemistry of nanobiomaterials (Elsevier, 2016); 2016. p. 163-91.

32. Shariare MH, Mondal TK, Alothaid H, Sohel MD, Wadud M, Aldughaim MS. Azithromycin nanosuspension preparation using evaporative precipitation into the aqueous solution (EPAS) method and its comparative dissolution study. CPA. CPA. 2021;17(9):1224-31. doi: 10.2174/1573412917999200909145745.

33. Chen X, Young TJ, Sarkari M, Williams RO, Johnston KP. Preparation of cyclosporine a nanoparticle by evaporative precipitation into an aqueous solution. International Journal of Pharmaceutics. 2002;242(1-2):3-14. doi: 10.1016/s0378-5173(02)00147-3, PMID 12176220.

34. Sinswat P, Gao X, Yacaman MJ, Williams RO, Johnston KP. Stabilizer choice for rapid dissolving high potency itraconazole particles formed by evaporative precipitation into aqueous solution. International Journal of Pharmaceutics. 2005;302(1-2):113-24. doi: 10.1016/j.ijpharm.2005.06.027, PMID 16109466.

35. Vaughn JM, Gao X, Yacaman MJJ, Johnston KP, Williams RO. Comparison of powder produced by evaporative precipitation into an aqueous solution (EPAS) and spray freezing into liquid (SFL) technologies using novel Z-contrast STEM and complementary techniques. European Journal of Pharmaceutics and Biopharmaceutics. 2005;60(1):81-9. doi: 10.1016/j.ejpb.2005.01.002, PMID 15848060.

36. Chen X, Lo CYL, Sarkari M, Williams RO, Johnston KP. Ketoprofen nanoparticle gels are formed by evaporative precipitation into an aqueous solution. AIChE J. 2006;52(7):2428-35. doi: 10.1002/aic.10848.

37. Kakran M, Sahoo NG, Li L, Judeh Z. Dissolution of artemisinin/polymer composite nanoparticles fabricated by evaporative precipitation of nanosuspension. Journal of Pharmacy and Pharmacology. 2010;62(4):413-21. doi: 10.1211/jpp.62.04.0002, PMID 20604829.

38. Bosselmann S, Nagao M, Chow KT, Williams RO. Influence of formulation and processing variables on properties of

itraconazole nanoparticles made by advanced evaporative precipitation into aqueous solution. AAPS PharmSciTech. 2012;13(3):949-60. doi: 10.1208/s12249-012-9817-0, PMID 22752680.

39. Balata G, Shamrool H. Spherical agglomeration versus solid dispersion as different trials to optimize dissolution and bioactivity of silymarin. Journal of Drug Delivery Science and Technology. 2014;24(5):478-85. doi: 10.1016/S1773-2247(14)50091-3.